An immunohistochemical study of lymphatic elements in the human brain

Éva Mezey[a,1], Ildikó Szalayova[a], Christopher T. Hogden[a], Alexandra Brady[a], Ágnes Dósa[b], Péter Sótonyi[b], and Miklós Palkovits[c]

[a]Adult Stem Cell Section, National Institute of Dental and Craniofacial Research, National Institutes of Health, Bethesda, MD 20892; [b]Department of Forensic Sciences, Semmelweis University, H-1091 Budapest, Hungary; and [c]Human Brain Tissue Bank, Semmelweis University, H-1094 Budapest, Hungary

Edited by Lawrence Steinman, Stanford University School of Medicine, Stanford, CA, and approved November 30, 2020 (received for review February 21, 2020)

Almost 150 papers about brain lymphatics have been published in the last 150 years. Recently, the information in these papers has been synthesized into a picture of central nervous system (CNS) "glymphatics," but the fine structure of lymphatic elements in the human brain based on imaging specific markers of lymphatic endothelium has not been described. We used LYVE1 and PDPN antibodies to visualize lymphatic marker-positive cells (LMPCs) in postmortem human brain samples, meninges, cavernous sinus (cavum trigeminale), and cranial nerves and bolstered our findings with a VEGFR3 antibody. LMPCs were present in the perivascular space, the walls of small and large arteries and veins, the media of large vessels along smooth muscle cell membranes, and the vascular adventitia. Lymphatic marker staining was detected in the pia mater, in the arachnoid, in venous sinuses, and among the layers of the dura mater. There were many LMPCs in the perineurium and endoneurium of cranial nerves. Soluble waste may move from the brain parenchyma via perivascular and paravascular routes to the closest subarachnoid space and then travel along the dura mater and/or cranial nerves. Particulate waste products travel along the laminae of the dura mater toward the jugular fossa, lamina cribrosa, and perineurium of the cranial nerves to enter the cervical lymphatics. CD3-positive T cells appear to be in close proximity to LMPCs in perivascular/perineural spaces throughout the brain. Both immunostaining and qPCR confirmed the presence of adhesion molecules in the CNS known to be involved in T cell migration.

podoplanin | meninges | CSF | T cells | cranial nerves

Lymph (named after the Roman goddess Lympha, meaning fresh water) was discovered by the ancient Greeks. Lymphatic glands, which are today called lymph nodes, were mentioned in a collection of writings that date to 300 to 500 BC (1), and lymphatic system (including the lymphatic vessels and nodes) was described in 1652 to 1653 by both Swedish (Olaus Rudbeck) and Danish (Thomas Bartholin) physicians. The first evidence that lymphatics might be present in the brain was published in 1787 (2) by Mascagni, an anatomy lecturer in Siena, Italy.

In 1869, Schwalbe demonstrated that tracer injected in the cerebrospinal fluid (CSF) space finds its way to extracranial lymphatics in dog. He concluded that the subarachnoid space (SAS) in the brain corresponds to lymphatics in the periphery (3). A direct connection (but not lymphatic vessels) between the SAS and nasal perivascular tissue was first demonstrated in humans by Key and Retzius (4) who injected tracers in the CSF space during autopsies. Tuke (5) suggested that waste material is moved from the human brain via the perivascular space (PVS). Since then, more than 150 studies have been published on the subject. Almost all of them described studies of rodents (see references in *SI Appendix*). The early studies were based on histology and what was known about peripheral lymphatics. Around the turn of the 20th century, members of two groups suggested that spinal "lymph channels" are not vessels with well formed walls but rather a continuous space around capillaries (6, 7). Zwillinger (8) showed that in humans there is a connection between the SAS and the lymphatic network in the nasal mucosa. This was generally accepted at the time [summarized in a later review by Jackson et al. (9)]. Connections between the SAS and the perineural space of the olfactory nerve and nasal lymphatic vessels in the lamina cribrosa were described in rabbits (10) and confirmed in a variety of rodents as well as in humans [see review by Koh et al. (11)].

Between 1960 and 1990, the second period during which work on CNS lymphatics flowered, a good deal of additional animal work was done without the benefit of the specific lymphatic markers that we have today. During this time, the phrases prevascular, perivascular, and paravascular were introduced to describe CNS lymphatics. Without the lymphatic markers, people still questioned the existence of a CNS "lymphatic" system. Among the important studies in this period, some were done by a group of Hungarian scientists. Földi et al. (12) described a "prelymphatic–lymphatic" pathway and said that it was perivascular (prelymphatic) until it reaches the jugular foramen where it meets individual lymphatic vessels around the internal carotid that later terminate in the deep cervical lymph nodes. They described the emergence of lymphatic vessels intracranially in the jugular foramen within layers of the dura mater. Csanda et al. (13, 14) found that following brain damage caused by implanting yttrium 90 in the brains of dogs, rabbits, cats, and rats, "Most of the breakdown substances of the brain tissue—originating especially

Significance

The connection between brain and peripheral lymphatics has been studied for 250 y, mainly in animals. Specific markers for lymphatic endothelial cells (LECs) were discovered about a decade ago. We stained postmortem human brains with LYVE1 and PDPN to identify LECs. Marker-positive cells were found in membranes covering the brain, walls of vessels, and perivascular spaces, and among nerve fibers. These spaces also seem to contain T cells and are connected to peripheral lymphatics through passageways in the nasal cavity, optic nerve, and base of the skull. Our findings show a path that brain waste products take when they leave the central nervous system, paths that may be bidirectional.

Author contributions: É.M. and M.P. designed research; É.M., I.S., C.T.H., and A.B. performed research; Á.D. and P.S. contributed new reagents/analytic tools; I.S. optimized technique for triple staining and tested all antibodies; C.T.H. prepared trigeminal cDNA, quality checked mRNA, and performed PCR; A.B. prepared cDNA from human brain samples and meninges and performed PCR; Á.D., P.S., and M.P. dissected postmortem samples and consulted neuropathological and forensic reports; M.P. added historic data; É.M. and M.P. analyzed data; É.M. and M.P. wrote the paper; and P.S. edited the paper.

The authors declare no competing interest.

This article is a PNAS Direct Submission.

[1]To whom correspondence may be addressed. Email: mezeye@mail.nih.gov.

This article contains supporting information online at https://www.pnas.org/lookup/suppl/doi:10.1073/pnas.2002574118/-/DCSupplemental.

Published January 14, 2021.

from myelin sheaths . . . are phagocytosed by microglial cells and transported to the vessel walls. In the remote vessels the lipid granules are . . . in the adventitia in half-moon like widenings that are also seen after cervical lymphatic blockade. . .. The migration of these substances tends to be toward the surface of the cortex. . .." Detailed reviews of research on lymphatics from earliest times through the middle of the 20th century were written by Cserr et al. (15), Földi (16), and Koh et al. (11). Recently, several workers have confirmed earlier findings and added new details using modern techniques.

For those who are interested, we have provided a supplementary reference list in *SI Appendix* showing many of the old as well as more recent references that we did not have the space to cite. We feel that the authors and their results deserve to be included in the history.

Finally, a third, new period of brain lymphatic research has begun. Investigators in the field have worked to demonstrate the existence of a functional flowing lymphatic system in the CNS using specific lymphatic endothelial markers. The most novel recent development was the discovery of the "glymphatic system," a waste clearance system composed of perivascular tunnels lined by the astrocytic processes that participate in forming the blood–brain barrier (BBB) (17–20). CSF travels through this system in the PVSs of arteries toward the PVSs of veins and moves waste products into the SAS and the venous sinuses (for review, see ref. 21). Johnston and colleagues (11, 22) described the role of the cavernous sinus (and other venous sinuses) in the absorption of CSF. In an extended review including fine imaging using structural MRI, Ramirez et al. (23) delineated the waste product movement and the possible clinical significance of any disturbance in these movements.

In 2015, two independent groups reported the existence of lymphatic vessels within the mouse dura mater (24, 25) using novel, specific lymphatic endothelial markers. Louveau et al. (25) stated that "these structures express all of the molecular hallmarks of lymphatic endothelial cells, are able to carry both fluid and immune cells from the cerebrospinal fluid and are connected to the deep cervical lymph nodes." In 2017, Reich's group used noninvasive MRI gadolinium imaging and following intravenous injection of the contrast agent visualized lymphatic vessels in human and nonhuman primate meninges (26). Ringstad and Eide (27) utilized MRI combined with CSF tracer, which was followed over time. They saw the tracer entering the dura parasagittally near the entry of cortical veins, concluding that there is transarachnoid passage of molecules and that the dura serves as a bridge between the brain and the peripheral lymphatic system. Meng et al. (28) used focal BBB disruption using magnetic resonance-guided ultrasound to demonstrate the contrast material distribution in the PVS, SAS, and the space surrounding large veins draining toward the dural sinuses in

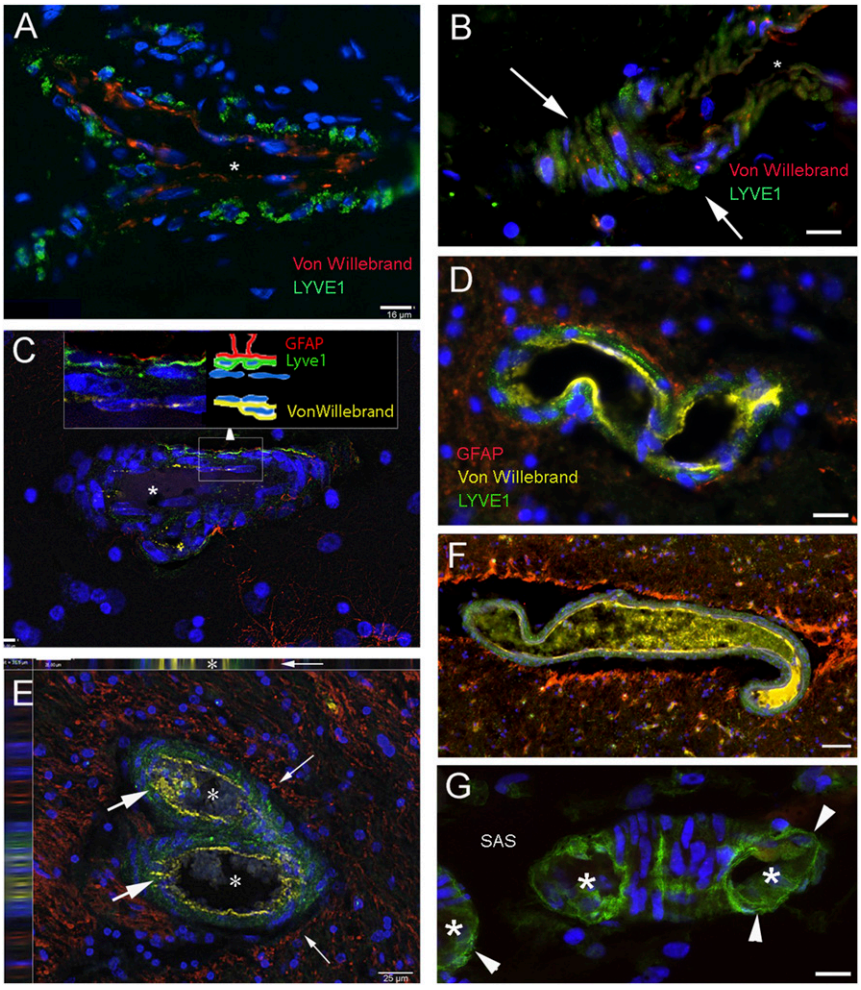

Fig. 1. LYVE1-labeled lymphatic cells along or within the wall of vessels in the human frontal and parietal cortex. Sections from brain regions of patients who suffered from neurological diseases (*A* and *C–F*) or who died from diseases that should not have affected the CNS (*B* and *G*) were immunostained using multiplex fluorescent immunohistochemistry with tyramide signal amplification (TSA). LYVE1, a membrane glycoprotein specific for lymphatic endothelial cells, is marked in green in all panels. The vascular endothelium is shown in red in *A* and *B* and in yellow in all other panels, representing the expression of von Willebrand factor. GFAP is stained in red for astrocytes forming the glia limitans around the vessels in *C–F*. *A–C* show small capillary-size structures that stained for LYVE1 and von Willebrand factor. DAPI, a chromosomal stain shown in blue, pinpoints cell nuclei in all images. The white arrows in *B* point at LYVE1-positive cells on the outside of the vessel before it has been transected by sectioning and the lumen becomes visible. In *C*, the image is a slice of a *Z* series taken at 0.5-μm intervals. The schematic *Inset* next to the enlarged (squared) area shows the layers stained with the different markers. (*D*) Three layers of cell types (capillary endothelium, lymphoid, and glial cells) stained with three different colors. *E* depicts a bifurcating vessel (lumina are labeled with asterisks), with LYVE1 labeling in the wall (large arrows) and lymphatic cells between basement membranes in the muscular layers. The image is one section out of a *Z*-stack and the side panels on *Top* and on the *Left* show the side views confirming the lymphatic-positive (green) staining lining the von Willebrand factor-positive vascular endothelium (yellow) on one side and a perivascular gap lined by red GFAP staining (small arrows). *F* is similar to *D* with the exception of the large artificial gap around the vessel. The yellow immunostained material in the lumen represents soluble von Willebrand factor; (*G*) a piece of a small capillary on the cortical surface with LYVE1-stained cells (arrowheads). Both in the cross-sections (labeled by asterisks) and the longitudinal portion, lymphatic cells form the outside wall. The star in *A–C* labels the lumina of the vessels. SAS, subarachnoid space. (Scale bars: *A*, *B*, *D*, *G*, 16 μm; *C*, 7 μm; *E*, 25 μm; *F*, 50 μm.)

humans. These elegant studies utilized specific lymphatic markers but had limited amounts of human data.

We looked in postmortem human brains (with and without neurological disease) for the presence of lymphatic endothelial markers (PDPN and LYVE1) to learn the routes that waste products can take from the interstitial space of the brain to the periphery. We analyzed the relationship between lymphatic marker-positive endothelial cells (LMPCs) and the vasculature of the brain parenchyma and meninges, and also explored the presence of lymphocytes in these spaces. Our goal was not to compare diseased brains to brains of subjects with no known neurological disease or to distinguish between different neurological diseases with regard to differences in the presence, location, or number of lymphatic elements. Indeed, we did not see any difference between subjects with or those without neurological disease in the distributions of the markers we used. What we describe in the paper are findings that seemed to be common to all the brains studied, were consistent, and did not differ in the 12 areas of the 10 brains we analyzed. This holds true for the presence and distribution of CD3-positive T cells that we show in the lymphatic spaces. In the brain parenchyma as well as in the meningeal spaces, we found T cells to be in close proximity to cells labeled with lymphatic markers in both normal and diseased brains.

We employed multiplex immunostainings using tyramide signal amplification (TSA) to localize the markers we used (29) and also performed PCRs to confirm the presence of the mRNA encoding them in one of the same samples that we used for immunocytochemistry (ICC). Given the nature of the study, we could not look at fluid movement in the spaces we describe but feel that the addition of morphological details in healthy and pathological human brains adds valuable information to what is already known mostly in nonhuman brains.

Results

Immunohistochemical Localization of Lymphatics throughout the Human Brain. We used LYVE1 and PDPN antibodies to visualize lymphatic endothelial cells. We could not locate a Prox1 antibody that would reliably allow us to visualize this nuclear lymphatic marker in postmortem samples. We attempted to also use an antibody to VEGFR3, a specific marker for lymphatic (vs. vascular) endothelium, to see if the receptors colocalize with the LYVE1 or the PDPN-positive elements but VEGFR3 is widely distributed in the brain parenchyma (30–33) and did not seem to be an ideal marker for this purpose.

Initially, we stained sections with LYVE1 and von Willebrand factor antibodies. The latter is used as a vascular endothelial marker (which also labels the soluble form of von Willebrand factor in the lumen of clogged vasculature), and we wanted to distinguish vascular from lymphatic endothelium (Fig. 1). Shrinkage of formaldehyde-fixed postmortem tissues causes artifactual gaps around vessels and lymphatic labeling was typically seen on one, but not both, sides of the resulting gaps.

We consistently found LYVE1-positive cells lining the PVSs around arteries and veins in cortical and subcortical human brain samples (Fig. 1 *A–G*). In Fig. 1*A*, a bifurcating vessel is clearly bordered by cells labeled with the antibody to LYVE1. Fig. 1*B* shows the outer wall of a small, transversely cut arteriole. LYVE1-labeled green cells are clearly seen outside the vessel wall. When astrocytes were also immunostained with GFAP, their processes appeared to be in close contact with the LMPCs (Fig. 1*C–F*) (also see the *Inset*). In the SAS, LYVE1 staining is apparent in the walls of small vessels (Fig. 1*G*). LMPCs are present in the middle layer (media) among smooth muscle cells in small arteries or collagen and elastic fibers in veins.

In all of the brain areas examined (cortex, hippocampus, striatum), astrocytic (GFAP) staining delineates the glia limitans and LYVE1 staining is visible within the adventitial layer of the vessels (Fig. 2 *A–E*). Fig. 2*D* shows a large artery with LYVE1 labeling in its adventitia and several small LYVE1-positive small arteries (vasa vasorum) that supply the large vessel. GFAP staining outlines the glia limitans formed by astrocytic feet that border the PVS.

We paid special attention to blood vessels entering and exiting the SAS (Fig. 3 *A–E*). When we examined single vessels on the cortical surface in serial sections, we found a few small LYVE1-positive channels that lacked vascular endothelial markers (Fig. 3*E*). We also found that arteries penetrating the cerebral cortex were associated with LYVE1-positive cells all along their paths (Fig. 3 *A–E*). All vessels in the SAS had cells with LYVE1-positive staining in their adventitia (Fig. 3 *C–E*).

The compact fibroblast/intercellular collagen periosteal portion of the dura contains lymphoid elements scattered on the wall of perforating vessels. In contrast, in the less compact inner (so-called meningeal) portion of the dura, small channels—interlaminar spaces—are outlined by LMPCs (Fig. 4 *A–D*), immunostained by both LYVE1 (Fig. 4 *A–C*) and PDPN (Fig. 4 *D* and *E*). One of these lymphatic channels is stained for podoplanin in the region of the falx cerebri of the dura mater in Fig. 4*E* (small arrows) in close proximity to a vessel (arrowheads) labeled by von Willebrand factor expression in green fluorescence. There are many LYVE1 (Fig. 4*F*) and PDPN (Fig. 4*G*)-positive cells associated with the cells of the arachnoid membrane (also called arachnoid barrier), and CD3-positive T cells can occasionally be found among them (Fig. 4*G*). Along the entire brain surface, cells of the pia mater are also positive for LYVE1 (Fig. 4 *G* and *H*). We suggest that the LMPCs around blood vessels originate from pia mater as it follows the brain surface and is "picked up" by vessels breaking the surface to travel toward the deeper parenchyma.

The cranial nerves also contained LMPCs. We found positive cells in the branches of the trigeminal nerves (Fig. 5 *A–D*), in and around the trigeminal ganglion and the cavernous sinus/cavum trigeminale sections (*Methods*) (Fig. 5*D*). This was also apparent in longitudinal sections of the trigeminal (Fig. 5*D*) and other cranial nerves including the glossopharyngeal, vagal, and accessory nerves (Fig. 5*E*, IX, X, and XI). A three-dimensional deconvolution of a *Z* series of a piece of the trigeminal nerve shows the fluorescent labeling of the endoneurium in Fig. 5*B*. Nerve bundles are encapsulated by connective tissue, called "perineurium." Sheets of similar tissue break up the large nerve bundles into fascicles. These sheaths are called the "epineurium." Within a fascicle, the contributing axons are myelinated, and single myelinated axons are surrounded by a sheath called the "endoneurium." In a cross-section of the trigeminal nerve, many of the myelinated axons were surrounded by LYVE1-stained cells forming the endoneurium (Fig. 5)

Presence of T Lymphocytes in Spaces Delineated by LMPCs. We wondered whether lymphocytes were present in the spaces delineated by LMPCs. To answer this question, we stained sections of the brain and trigeminal ganglion with an antibody to CD3, a specific T lymphocyte marker. In all of the brains we studied, we found extravascular lymphocytes in the brain regions we examined. Fig. 6 shows vessels and trigeminal ganglion with CD3-positive cells. Fig. 6*A* shows a large vessel in the amygdala with many CD3-positive cells between the outer wall of the vessel and the LYVE1-positive cells lining the PVS. Similarly, many CD3-positive T lymphocytes were visible around blood vessels (in PVSs) in the hippocampal sulcus (Fig. 6*B*), striatum (Fig. 6 *C* and *H*), inside and around the cavernous sinus and cavum trigeminale (Fig. 6 *E* and *F*), and on the surface of the parietal cortex (Fig. 6*D*). Fig. 6*G* shows a cross-section of a small artery in the amygdala, where CD3-positive T cells are clearly visible in the PVS attached to LYVE1-positive cells on the surface of the vessel and at the other side of the artificial gap. Fig. 6*H* shows a

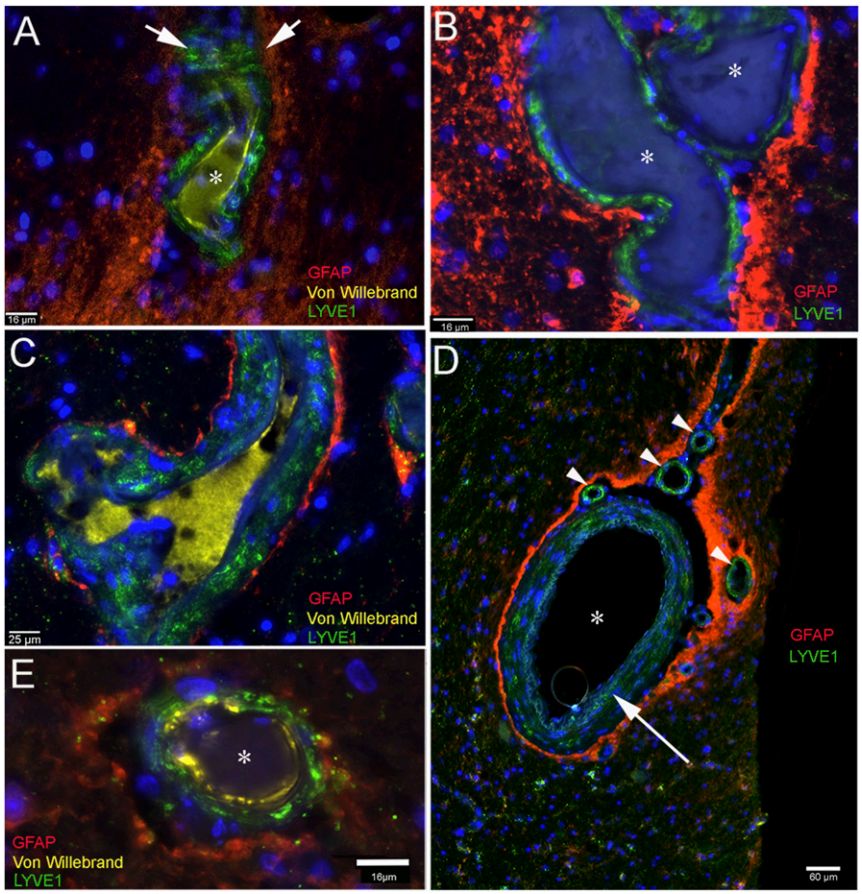

Fig. 2. LYVE1-positive cells in vasculature in several brain regions; the glia limitans labeled by GFAP staining outlines the parenchymal side of the PVS. Multiplex immunostained sections from a variety of brain regions from patients. Red fluorescent processes of astrocytes (glia limitans) surround a small artificial space around the vessels. LYVE1 is stained in green and show the LMPCs that are present in the vascular adventitia in all panels. *A* and *B* show the von Willebrand factor staining in the vascular endothelial cells and also its soluble form in the vascular lumen (*A* and *C*). The green LYVE1-positive cells are dispersed among the muscle cells of the vascular wall. *C* shows a part of venous vasculature, clearly labeling cells in the wall with green (LYVE1) and the glia limitans (GFAP) in red. In *D*, a large artery can be seen (asterisk) with positive intralaminar LYVE1-labeled cells in the muscular layer (long arrow) among the basement membranes. The red staining represents the glia limitans that surrounds the artery and also the small LYVE1-stained vessels (vasa vasorum) in the adventitia. *E*, Similar to *A*–*C*, but observe the large artificial gap around the vessel. (Scale bars: *A*, *B*, and *E*, 16 µm; *C*, 25 µm; *D*, 60 µm.)

vascular loop in the striatum, where numerous T cells are attached to the LYVE1-positive outer surface. Similarly, Fig. 7*A* shows an overlay of CD3-positive T cells (Fig. 7*B*) attached to the PDPN-positive surface of a large vessel within the parenchyma (Fig. 7*C*). A process formed from a chain of PDPN-positive cells can be seen in Fig. 7*D*. Many green CD3-positive T cells (arrowheads) are attached to the membrane (arrows) of the LMPCs. We looked for the presence of ICAM1, an adhesion molecule that is thought to play a role in T cell migration, in the trigeminal nerve (Fig. 7*E*) and found that the CD3-positive T cells are adjacent to cells expressing this adhesion molecule. In the ganglion itself, we saw that the membranes of the satellite cells around some ganglion cells were strongly positive for PDPN and many CD3-positive T cells were in close proximity to the PDPN-positive cell membranes (Fig. 7 *F*–*H*). We performed triple staining to look for adhesion molecules that could be involved in T cell mobility in nervous tissue. In the trigeminal ganglion, the satellite cells that form a ring around the large ganglion cells all stained positive with PDPN (Fig. 7 *F*–*H*) and were in close contact with CD3-positive T cells. ICAM1 staining was found around some of the ganglion cells, but in these cases the antibody stained all of the satellite cells surrounding the neuron (Fig. 7 *G* and *H*) and colocalized with PDPN (Fig. 7*H*).

T cell accumulation was seen where nerve branches were cut (Fig. 8*A*), suggesting their presence in the perineural space. LYVE1 and PDPN colocalized in cells and processes of the nerve bundles and T cells were always in close proximity to these LMPCs (Fig. 8*B*). Within the nerve bundle, where T cells accumulated among the PDPN-positive cells, ICAM1 was also highly expressed (Fig. 8 *C* and *D*). A section of the trigeminal ganglion and branches of the fifth nerve are shown in Fig. 8*D*. PDPN staining often surrounds the ganglion cells (some of which are labeled by stars) and is also found around and within nerve bundles of the fifth cranial nerve (labeled by V). Many CD3-positive T cells are visible in all of these areas. ICAM1 is also present in a portion of PDPN-positive cells and processes surrounding the ganglion cells. In the trigeminal ganglion cells and branches of the trigeminal nerves, T cells were also present in all of the samples we examined, but we saw an especially large number in two people who died of self-inflicted strangulation (*SI Appendix*, Fig. S1 *A–D*). As a control for the immunohistochemistry, we looked for and found colocalization of LYVE1 and VEGFR3. The latter is another known lymphatic endothelial marker (*SI Appendix*, Fig. S2). We performed TSA amplification in the absence of a primary antibody (*SI Appendix*, Fig. S3) as a negative control for staining. Finally, the specificity of the LYVE1 antibody was also confirmed by demonstrating that it is also expressed in barrier-associated macrophages (*SI Appendix*, Fig. S4) that can be specifically labeled by CD163, as described in the literature (34).

PCR to Confirm the Presence of Protein mRNAs. To validate the immunohistochemical studies, we used qPCR to look for mRNAs encoding the antigens that we had detected. For this purpose, we obtained tissue of the pia mater, dura mater, cortical samples used for immunostaining and three trigeminal ganglia and nerves from the Maryland Brain Bank and prepared RNA from them. We looked for the presence of PDPN, LYVE1, VEGFR3, PROX1, ICAM1, VCAM1, and L-Selectin (CD62-L). The highly specific SYBR Green primers revealed that the mRNAs were moderately to highly abundant in all brain and ganglion samples tested. The results are shown in Fig. 9 and expressed as fold changes compared to the housekeeping gene (HPRT).

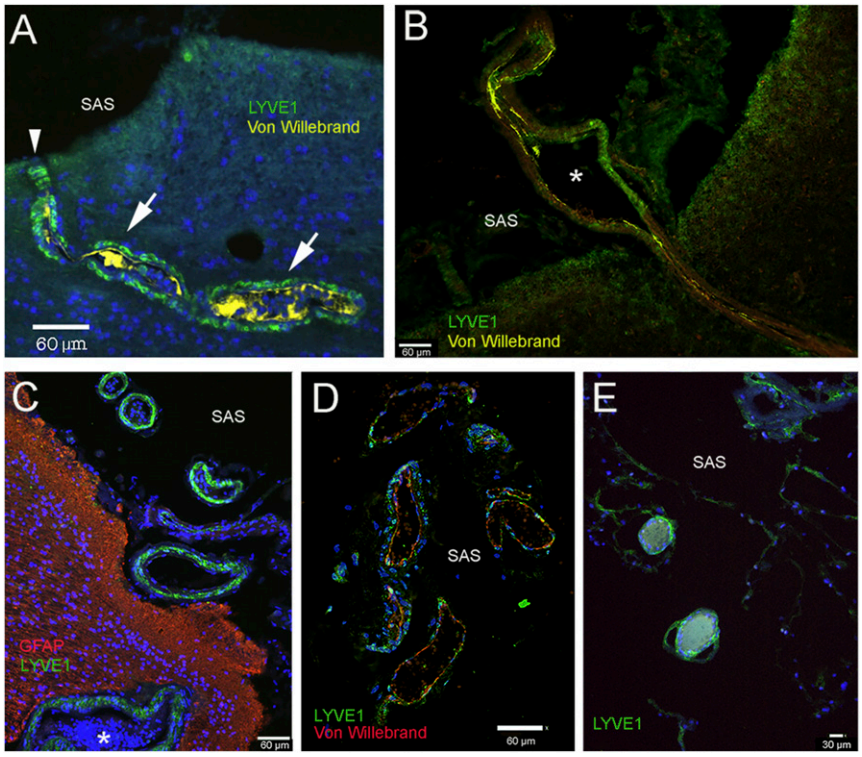

Fig. 3. Lymphatic markers in the wall of vessels connecting with the subarachnoid space (SAS) over the frontal and parietal cortex. *A–C* and *E* are taken from patients with underlying neurological diseases, and *C* is from a patient with no neurological disease. *A* and *B* show vessels in the frontal cortex connecting with the subarachnoid space (SAS) in the arachnoid trabeculae. The outsides of the vessels are delineated by LYVE1-positive green cells, while the vascular endothelium is in yellow (staining von Willebrand factor). In *A*, the green LYVE1-positive cells that follow the vessel are labeled with arrows. The entry point of the vessel at the border of the SAS is labeled with an arrowhead. *C–E* show vessels in the SAS. In *C*, the outside wall of the vessel is LYVE1 positive (green), and processes of astrocytes (GFAP) at the surface of the brain are red. The asterisks in *B* and *C* label vascular lumina. (Scale bars: *A–D*, 60 μm; *E*, 30 μm.)

Discussion

We studied and described the distribution of specific markers of lymphatic endothelial cells in tissues of the human brain and spinal cord. We did this to learn how interstitial fluid in the brain might reach the dura and the SAS. We believe that the outflow pathways converge on cranial and spinal nerves and end in the regional lymphatics as soon as they exit the cranial vault. This pathway allows the brain to rid itself of waste products and ensures an outflow for the continuously produced CSF.

There is confusion in the literature with regard to the nomenclature of spaces between the vasculature and the parenchyma of the brain. The pia mater follows arteries into the brain parenchyma and forms a continuous one-cell-thick layer. This layer is permeable to solutes and immune (but not erythroid) cells that can pass through it (35). The pial covering of capillaries is incomplete (36, 37). The vasculature is separated from the pia by the endothelial basement membrane (including scattered pericytes) among smooth muscle cells in larger vessels, as well as by the glia limitans, formed by astrocytic processes around vessels (38).

Lymphatics and the PVS. PVSs were first described by Pestalozzi in 1849 (39) and then by Virchow in 1851 (40) and Robin in 1859 (41). Today, these are referred to as Virchow–Robin spaces (VRSs). Arterial and venous PVSs surround the cerebral perforating vessels, from the SAS to their intraparenchymal route. These spaces contain interstitial fluid and are involved in the clearance of fluids and metabolic waste from the brain. They have recently been relabeled the glymphatic system (19).

In 1910, Mott et al. (42) suggested that there is a lymphatic sheath around vessels in the brain that is continuous with the adventitia and made of fusiform cells. This sheath forms the vascular surface of the PVS and its outer side is delineated by the pia mater covering the neural tissue. He called this a contiguous system of perivascular lymphatics. These spaces seem to be similar to the "true perivascular spaces" described by Woollam and Millen in 1955 (43).

Cserr et al. in 1976 (44) pointed to the importance of PVSs in interstitial fluid movement and compared the brain PVSs to the lymphatics of other organs. Földi et al. (45) described a system of interconnecting channels that surround cerebral vessels and said these intracranial "prelymphatics" drain into the extracranial lymphatics (13, 16) separated by valves in the jugular foramen. Experimental results described by Csanda et al. in 1983 (13) showed that injecting blood into the cisterna magna of dogs results in the accumulation of red cells in the upper part of the superior cervical lymph node, and postmortem samples from patients obtained 2 wk after they died from subarachnoid bleeds showed the presence of hemosiderin in the cervical lymph nodes (13). A similar path was confirmed in dogs by tracing sudanophil breakdown products following the implantation of a radioactive yttrium rod into the brain (46).

In the last decade, a renewed interest in brain lymphatics has brought them to the fore again. The Needergard group, describing their glymphatic hypothesis, suggested that there is a brain wide pathway between the vasculature and the feet of astroglial cells to clear interstitial waste from the brain parenchyma. The waste ultimately will be directed toward the cervical lymph nodes and vessels (see review in ref. 21).

Lymphatic vessels have been described in the human dura mater by Andres et al. in 1987 (47) and recently confirmed by Aspelund et al. (24) and Louveau et al. (25). Authors of a recent study used MRI imaging of humans and looked for clearance pathways in vivo. Following intrathecal administration of a contrast material, they concluded that the parasagittal dura next to the superior sagittal sinus serves as a bridge between CSF in the brain parenchyma and the dural lymphatic vessels (27).

Our findings show that the "perivascular" space described by many earlier investigators appears to consist of endothelial cells that express most of the same markers that peripheral lymphatic endothelial cells have: LYVE1, PDPN, VEGF3, and Prox1, a transcription factor (48). LYVE1 is a type I integral membrane glycoprotein. It binds to soluble and immobilized hyaluronan.

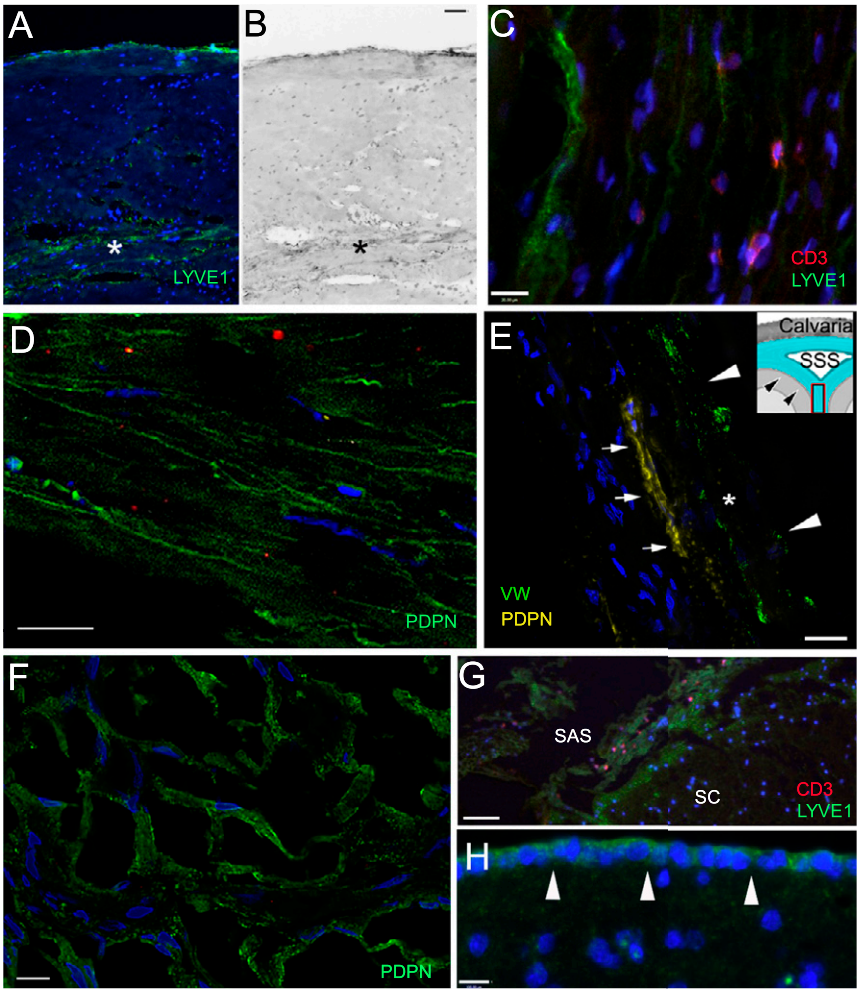

Fig. 4. Lymphatic markers (LYVE1 and PDPN) in the meninges. Sections of the meninges from persons died of nonneurological causes (*A*, *B*, and *E–G*) and who suffered from neurological disease (*C* and *D*). (*A–D*) Upper (periosteal) and lower meningeal segments of the dura mater from the sagittal sinus; (*E*) falx cerebri; (*F* and *G*) arachnoid; (*H*) pia mater. (*A* and *B*) Bright-field image of the same field; in the dura mater LYVE1-positive lymphatic channels are stained green. The inner periosteal layer of the dura is adherent to the periosteum of the cranium. This layer is composed of tough compact collagenous fibers. The meningeal layer (labeled with a star) faces the arachnoid membrane. This layer is less compact; blood vessels and lymphatic elements fill up the intermembranous spaces. The capillaries and postcapillary venules are fenestrated (no BBB). (*C*) LYVE1-positive lymphatic cells and scattered T cells (stained in red with CD3 antibody) can be seen among the collagenous membranes of the dura. *D* shows podoplanin (PDPN; another accepted marker of lymphatic endothelial cells) positivity (green) in the dura mater in the inner surface of the basis of the cranium, in the cavernous sinus. *E* demonstrates a PDPN-positive (yellow fluorescence) lymphatic channel (small arrows) next to a sectioned vessel labeled with an asterisk and arrowheads (vascular endothelium is positive for von Willebrand factor; green fluorescence) in a thin section (taken from a *Z* stack at 1-μm optical thickness) of the falx cerebri (the anatomy is shown in the *Inset*, where arrowheads point at the dura mater and the square shows the approximate area of the falx cerebri where the sample was taken from. *F* demonstrates podoplanin staining of the arachnoid (from the Greek word for spider). It resembles a spider web. In *G*, many LYVE1-positive epithelial cells can be observed in the arachnoid covering the spinal cord (SC) and red fluorescent CD3-positive T cells are occasionally present near the LYVE1-positive connective tissue cells. (*H*) The cells of the pia mater (pointed at by white arrows) on the surface of the frontal cortex express LYVE1 (green). SAS, subarachnoid space; SSS, superior sagittal sinus. (Scale bars: *A* and *B*, 100 μm; *C–F*, as labeled.)

Podoplanin is a glycoprotein that belongs to the mucin-type protein family. We mainly relied on LYVE1 and PNPN as markers because VEGFR3 is too promiscuous and Prox1 proved too hard to detect. We found LYVE1 and PDPN-positive cells in all brain regions we examined. The two antibodies seemed to stain the same cells, but the antigens had different intracellular distributions. The same cells were also VEGFR3 positive, but many additional ones were stained by this antibody. All vascular cross-sections were surrounded by cells positive for lymphatic markers. We observed perineurial and endoneurial staining in longitudinal and cross-sections of nerve bundles, around satellite cells of the trigeminal ganglion, in the dura mater, in vessels in the SAS, in cells of the pia mater, and in the adventitia of large vessels in many brain regions.

T Lymphocytes in the Brain Perivascular Spaces. After we found lymphatic elements in the human brain, we looked for the presence and distribution of T lymphocytes there to determine whether lymphatic endothelial cells and lymphocytes in the CNS are associated with one another. Immune cells are known to monitor the CNS for danger signals and play a role in restoration of CNS homeostasis (49). Peripherally derived T cells, macrophages, and dendritic cells all appear to participate in this. Since 80% of the CNS sentinel cells are T cells, we used CD3 to look for these cells initially. T cells can enter the CNS in any of three ways. They can get into the CSF through the choroid plexus, through the Virchow–Robin space, or through postcapillary venules (50). These perivascular lymphocytes are thought to screen the CSF for potentially harmful molecules (50–52). Cserr and her group (53) were the first to demonstrate that infusing an antigen into the CSF space will activate the peripheral immune system, suggesting a direct connection between the SAS and the periphery. While a number of investigators have described immune cells in the brain associated with pathologic conditions, much less information is available regarding the presence and function of T cells there in the absence of disease. Few lymphocytes are present in the healthy brain, and most of these are effector and central memory T cells (54).

After Cserr published her paper, members of other groups reached a similar conclusion after they injected a variety of bacterial and viral agents into the brain parenchyma (see ref. 55). A few recent excellent reviews summarize what is known about the roles of immune cells in the CNS in health and disease and the cellular and molecular mechanisms regarding lymphatic drainage and cell trafficking in the CNS (38, 56). We observed that CD3-positive T cells were present in the PVSs of large vessels, in the adventitia of the vasculature, and among the cells of the of the arachnoid membranes. We also found a surprising number of T cells among the cells of the Gasser (trigeminal) ganglion and under the epineurium, in the perineurium, and among the axons within the nerve of the branches of the trigeminal nerve.

The movement of T cells within the PVSs is thought to be determined by the expression of appropriate adhesion molecules by endothelial cells. We did a small preliminary screen to see whether the lymphoid epithelial cells in the human brain express

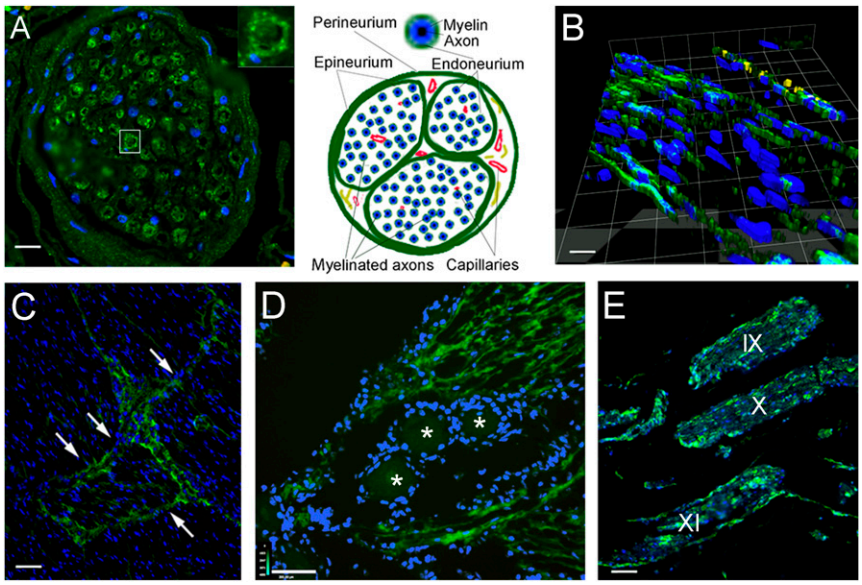

Fig. 5. Lymphatic endothelial markers among the nerve fibers and fascicles of cranial nerves. Sections stained with antibody to LYVE1 (visualized in green fluorescence) of cranial nerves and the trigeminal ganglion from persons deceased without known neurological disorders. (*A*) Cross-sections of a branch of the trigeminal nerve are shown. Interestingly, the endoneurium (connective tissue sheets around the individual myelinated fibers) is positively stained; the *Inset* shows an enlargement of a single nerve fiber enclosed by the LYVE1-positive endoneurium. Nuclei of glial cells (Schwann cells and possibly microglia) and connective tissue are visible in blue (DAPI). In *B*, a three-dimensional reconstruction of a section of the trigeminal nerve is shown, demonstrating the presence of longitudinal LMPCs among the nerve fibers. On the *Top* of the image, cells with yellow fluorescence express the von Willebrand factor, indicating vascular endothelial cells of a small vessel in the section. (*C*) In a cross-section across a large nerve bundle, labeling is very strong among the fascicles (arrows). (*D*) A section through the trigeminal ganglion is shown. Cross-sections of trigeminal fibers around the ganglion cells (labeled with stars) show strong LYVE1 labeling. (*E*) Section of the brainstem with the origin of the IX, X, and XI cranial nerves running parallel. The perineurium as well as cells among the myelinated axons within the nerve fibers are strongly labeled with LYVE1. (Scale bars: *A*, 50 μm; *B*, 25 μm; *C* and *E*, 110 μm; *D*, 130 μm.)

adhesion molecules that are known to be used by T cells in their transepithelial movements. We stained brain sections with VCAM1, ICAM1, and selectin IL62. The endothelial cells that expressed lymphatic markers were not VCAM1 or selectin positive, but they did express ICAM1, an adhesion molecule that binds to LFA1 and is expressed in over 60% of T cells isolated from human CSF (57). It has also been shown in vitro using mouse brain endothelial cells that the cytoplasmic tail of the endothelial ICAM1 is essential to support trans endothelial migration of T lymphocytes (58).

Lymphatic Drainage of the Human Brain. Regarding lymphatic "drainage" from the human brain, it has long been suggested that cranial nerves leaving the parenchyma might serve as one possible connection between the CSF space and the peripheral lymphatic system. Schwalbe was the first in 1869 to suggest that intrathecally injected tracers appear in the lymph nodes (3). Key and Retzius (4) demonstrated the connection between the CSF space and the nasal mucosa. For a detailed review, see ref. 13.

Bruce and Dawson (6) reviewed the information that was available about spinal lymphatic spaces in 1900. They highlighted the pioneering works of His (1875), who first suggested that the main route for brain interstitial fluid flow is the PVS. Subsequently, Key and Retzius (4) and Obersteiner (7) concluded that "the tissue lymph spaces discharge everywhere into the PVS and the lymph flows out in the direction of the periphery of the cord." Both the cranial and spinal nerves leaving the CNS are surrounded by a cuff of the SAS where the contacting meninges form a funnel-shaped space that acts like a valve: When outside pressure is high, it closes (10). Cserr's group described the drainage of CSF through outflow pathways along certain cranial nerves and spinal nerve roots and concluded that "a new view of CNS immunology should incorporate continuous and highly regulated communication between the brain and the immune system" (15).

In our studies, we analyzed the trigeminal system in samples of the cavernous sinus–cavum trigeminale samples. In all the samples we looked at, there are occasional CD3-positive T cells around ganglionic cells and large nerve bundles under the epineurium, between the fascicles, under the perineurium, and in the endoneurial space. We found that the epineurium, the perineurium, and the endoneurium (connective tissue lining individual myelinated fibers) were all positive for lymphatic markers as well as the adhesion molecule, ICAM1. The T cells that we saw were always in close proximity to cells that expressed lymphatic markers and the adhesion molecules. We hypothesize that T cells might move in these spaces just as they "roll" on endothelial cells and that they are likely to engage in surveillance of the CNS environment. Their movement could be orchestrated by the synchronized expression of the adhesion molecule by the lymphoid epithelial cells and its cognate ligand LFA1, produced by the immune cells. This might result in a slow "flow" of immune cells along the nerves in the PVSs. The cells might be gently pushed along by the movement of interstitial fluid/CSF around the vasculature or by endoneurial fluid flowing among the fibers in cranial/peripheral nerves (24, 59). It has already been suggested that ICAM1 might play a significant role in the migration of T cells within the CNS (60, 61). Neutralizing antibodies to ICAM1 and LFA1 impair the ability of T lymphocytes to cross endothelial barriers in the CNS (58, 62). In samples from two people who died by self-inflicted strangulation, we noticed a very high number of T cells along the nerve branches of the fifth nerve compared to two people who died following a drug overdose and traffic accident, respectively. The pileup of the cells above the line of strangulation suggests a directional movement of the T cells within the nerve that was blocked by the strangulation (*SI Appendix*, Fig. S1).

These results fit well with previous data by Csanda et al. showing that experimental cervical lymphatic blockage in dogs results in cerebral edema (63) and Cserr's hypothesis that there is a possible outflow of CSF/solutes along the cranial nerves toward the peripheral lymphatics (15). In an elegant recent study, Ahn et al. (64) called attention to the importance of the basal (as opposed to dorsal) meningeal lymphatic vessels in CSF drainage. Although he studied mice, the observation seems to be consistent with our human data with special emphasis on the potential role of the cavernous sinus connecting the CSF space to the lymphatics in the pharyngeal area. Goldman et al. (65) described the trafficking of T cells from the brain toward the nasal mucosa through the cribroid plate on route to the cervical lymph nodes. Regarding the available routes for CSF drainage from the CNS toward peripheral lymphatics, it is important to mention the cranial foramina, the openings in the base of the

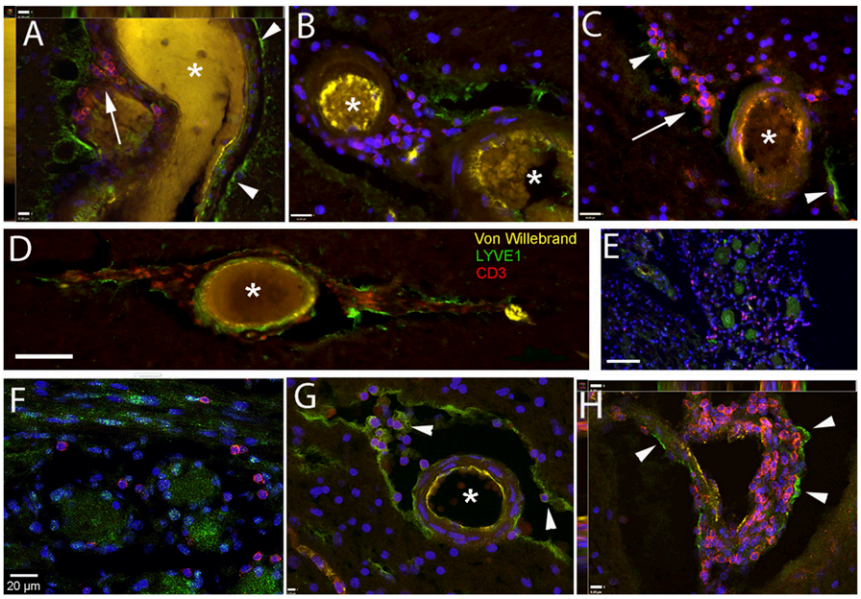

Fig. 6. T lymphocytes identified adjacent to LYVE1-positive staining in the PVSs. Sections from persons who suffered from neurological diseases (*A*–*D*) and without known neurological diseases (*E*–*G*). Samples were taken from the amygdala (*A* and *G*), parietal cortex (*D*), trigeminal ganglion (*E* and *F*), striatum (*C* and *H*), and vessels in the hippocampal sulcus (*B*). In all of the images, the asterisks label vascular lumina, arrows point at a congregation of T cells, and arrowheads point at some of LYVE1-positive cellular membranes. *A* shows the cross/longitudinal section of a large vein, where the vascular endothelium is yellow (VW: von Willebrand), the brain surface is lined by LYVE1-positive green cells, and the space between the outside of the vessel wall and the LYVE1-positive surface is filled with a large number of red, CD3-positive T cells. The image is one level of a *Z* stack showing the side views on the *Top* and *Left*. *B* shows similar images with small arteries in the hippocampal sulcus (*B*), and in the striatum (*C* and *H*). Once again, the T cells are in close proximity to LYVE1-positive structures. (*E* and *F*) High and low magnification, respectively, of the trigeminal ganglion, where CD3-positive T cells are found in-between the ganglion cells and—similarly to the other pictures—are close by to long LYVE1-positive cells in the connective tissue. *G* shows a cross-section of a medium-size artery, with VW staining in yellow, where LYVE1-positive cells are lining both the brain parenchyma and the outside of the vessel. They are also present within the adventitia of the vessel. The space between the brain and the vessel is filled with T cells (red), a few attached to the outside of the vascular wall. *H* shows a vascular loop in the striatum completely covered with T cells. The image is one level of a *Z* stack showing the side views on the *Top* and *Left*. (Scale bars: *A*, *G*, and *H*, 9 μm; *B* and *C*, 16 μm; *D*, 90 μm; *E*, 80 μm; *F*, 20 μm.)

skull that cranial nerves and vessels pass through to reach areas with a dense peripheral lymphatic network containing 20 to 30 lymph nodes. These include the cribriform plate (olfactory nerve), the optic canal (optic nerve), foramen rotundum (maxillary nerve), foramen ovale (mandibular nerve), and the jugular foramen, where the glossopharyngeal, vagal, and accessory nerves leave the cranium and the foramen lacerum that connects the extracranial pterygoid plexus with the intracranial cavernous sinus.

In humans, a need for such outflow routes is supported by the fact that there is 340 to 500 mL of CSF produced daily. At any given time point, there is 140 mL of CSF inside the skull, 30 mL of which is in the ventricular system and 110 mL in the SAS. This is completely replaced three times a day (66). Although they were based on a very small sample (two strangled vs. two subjects who died of natural causes), our observation that there is an increased number of T cells in the trigeminal ganglion and nerve branches of subjects who died of self-inflicted strangulation suggest a possible directional movement of immune cells from the CNS space toward the periphery. The magnitude of the cellular accumulation may depend on many factors, such as the length of the agonal period, the circumstances of death, and the health of the vasculature. More work will be needed to understand this phenomenon. Lymphatics in and around the cranial nerves [and spinal nerves (15)] play an important role in transporting neuronal end products out of the brain. Each cranial nerve is encapsulated by meninges until it reaches the appropriate foramen through which it leaves the cranial vault. Thus, lymphoid elements carried in the SAS, the meningeal portion of the dura, and the perineural space may reach cervical lymph vessels in the nasal cavity via the olfactory, optic, or trigeminal nerves.

A recent report focused on whether the CNS–lymphatic connection might be the basis of an antigen-specific immune response evoked by T cells traveling from diseased brain areas to the cervical lymph nodes. It seems to support our findings of T cell movement toward the cervical lymphatics. In a mouse model of glioblastoma, the authors demonstrated that ligation of the upper cervical lymph nodes results in a significant decrease in survival (67).

Using trigeminal ganglia from three different donors (Maryland Brain Bank) and samples from cortex, pia mater, and dura mater, we performed qPCR to detect mRNAs encoding the proteins that we visualized using antibodies and amplified immunostaining. The adhesion molecule mRNAs that we attempted to detect (ICAM1, VCAM1, and L-selectin) were all expressed in the tissues examined (Fig. 9). We were only able to successfully stain cells with LYVE1, PDPN, VEGFR3, and ICAM1 antibodies, however. The discrepancy could have to do with the ability of the available antibodies to bind to antigens in paraffin-embedded postmortem human material. It is also possible, but less likely, that the mRNAs are not translated into protein in sufficient amounts to be detected.

Our study is based mainly on morphology, with added analyses of brain samples for expression of mRNAs encoding the proteins we studied. The qPCR studies were intended to support the conclusion that the proteins we detected using amplified immunostaining are indeed expressed in tissues examined. Most of the findings align well with old (and sometimes ancient) literature data (see *SI Appendix*, list of historical references along a timeline) and show that, in addition to dural lymphatic channels, there is a perivascular network in the human brain that enables solutes, cells, and extracellular fluid to travel from the parenchyma extracranially, and eventually to move toward venous sinuses and the peripheral (cervical) lymphatic system (68). In his Morisonian Lecture in 1894, Tuke (69) made a similar suggestion saying that "each vessel carries with it a prolongation of the pia, which surrounds the vessels to its ultimate branches. This is often spoken of as the adventitia of the vessel. From this pial or hyaline sheath, processes are given off which encapsulate the cells, each of which is thus surrounded by a perivascular capsule" (5, 70) (*SI Appendix*, Fig. S5). According to our results, this space contains T cells neighboring surfaces that express lymphatic markers. Our preliminary results show that most of these T cells are CD4 lymphocytes. When we used CD45, a marker of all white cells, we noticed that not all the cells stained for CD45

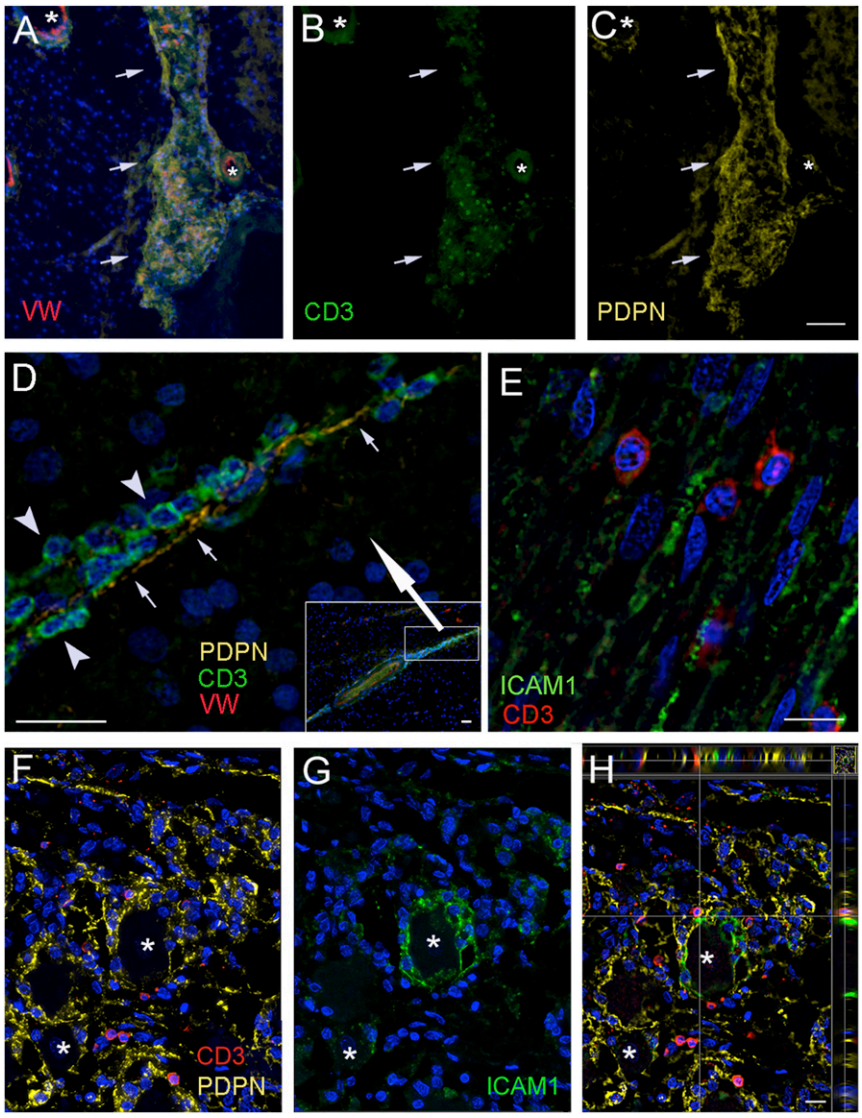

Fig. 7. Confirmation of findings with a second lymphatic element marker, podoplanin. Sections from persons who suffered from neurological disease (*A–D*), or without known neurological diseases (*E–H*). Samples were taken from the basal ganglia, the parietal cortex, and the cavernous sinus including the trigeminal ganglion and nerves. *A–C* are images of the same area using different fluorescent filters. *A* shows the overlay of nuclear DAPI (blue); in *B*, T cells labeled with CD3 (green) and vascular endothelium shown by an antibody to von Willebrand factor (red) and the lymphatic endothelial marker, podoplanin (yellow) in the globus pallidus. The outside of a vessel within the parenchyma is visible that is (*B*) covered with green fluorescent T cells (CD3) that are attached to (*C*) the podoplanin-positive (yellow) outer membrane. The asterisks label vascular lumina; the arrows point at the vascular loops within the parenchyma (the DAPI staining in *A* shows the presence of neuronal cells, while in *B* only the T cells are visible). *D* shows a continuation of a perivascular space (seen in the *Inset* in the *Lower Right* corner) enlarged (see the rectangle in the *Inset* with the large white arrow pointing to the enlarged area) where CD3 positive green T cells (arrowheads) can be observed attached along the podoplanin positive (yellow) membranes (small arrows) of endothelial cells. *E* is a section of a branch of the trigeminal nerve, where the adhesion factor ICAM1 is stained green and red T cells are attached to the ICAM1-positive fibers. *F–H* demonstrate a portion of the trigeminal ganglion with ganglion cells (asterisks) to show the overlap of PDPN (yellow), ICAM1 (green), and the CD3-positive T cells (red) adjacent to both. It is interesting that ICAM1 (*G*) is expressed by satellite cells surrounding the ganglion cells, but only around a fraction of the neurons. In *H*, which is an optical slice of the section, the side panels clearly indicate the close proximity of green (ICAM1-expressing) and yellow (PDPN-expressing) structures to the red T cells. (Scale bars: *A–C*, 75 μm; *D*, 30 μm, *D* (*Inset*), 25 μm, *E–H*, 20 μm.)

were CD3 positive. Some were probably macrophages, which are also present in these spaces (50). We cannot say anything about how CSF flows through the brain lymphatic system based on our observations of postmortem human material, and we have not tried to relate our data to the glymphatic hypothesis (71). Since the PVSs lack the valves that peripheral lymphatic vessels have, solutes might move either to or from the brain based on fluctuations in pressure (18). Thus, breakdown products of dead cells, tissue fragments, or protein aggregates may travel out of the brain, and immune cells or pathogens might move to or from the brain along the same pathways. The possibility of such directional movement of pathogens (*Listeria*) in the branches of sheep trigeminal nerves was suggested by Charlton and Garcia in 1977 (72). Our observation of LMPCs within the trigeminal system is consistent with this suggestion.

Recently, more data became available on the possible glymphatic system in the human brain: Thomas et al. (73) summarized the experimental results on fluid dynamics of the CSF in PVSs and their role in clearing waste products from the CNS. Most studies suggest a role of arterial pulsation in the movement of materials in the PVS. Raz et al. (74) analyzed iodine leakage from vessels following endovascular perforations during thrombectomies using serial CT images in humans. Their observations are in agreement with the existence of the glymphatic (or a similar perivascular pathway) system in humans. Similar conclusion was reached by Meng et al. (28) who used ultrasound induced opening of the BBB followed by injection of contrast material. They describe the patterns of the distribution of the contrast material in the PVSs, in the SAS, and in large veins that drain the dural sinuses. In another recent study (75), the space between the pia mater surrounding the walls of cortical veins is enhanced and connects the dural lymphatics along the superior sagittal sinus, ensuring a possible outflow from the glymphatic system.

Additional studies will be needed to discover the function of the lymphatic system in the human brain, the character and composition of the immune cells present in the CNS lymphatics in health and disease, and the signals that play a role in the interactions between the LMPCs lining these spaces and the cells moving in them. Our findings also show that hard-working, disciplined, and insightful anatomists and clinicians in the past who did not have the benefit of modern methods were still able to recognize and describe the lymphatic spaces in the brain. We should all learn from this.

Methods

Brain and Ganglion Samples. Anonymized postmortem human brain samples were obtained from several sources: the Harvard Tissue Bank at McLean Hospital (paraffin sections) and the Department of Forensic Sciences of

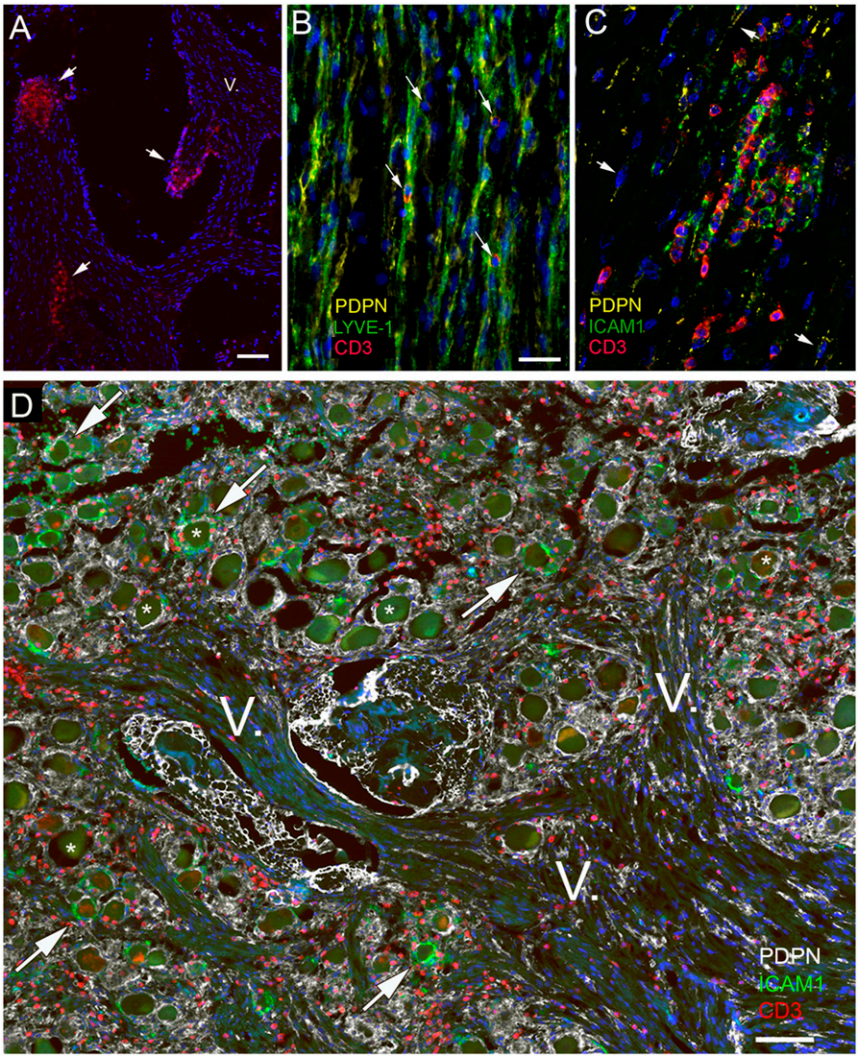

Fig. 8. Expression of adhesion molecules in relation to T cells and lymphatic markers in the trigeminal nerve. All panels are from subjects with no known neurological disease. The trigeminal nerve was stained for CD3 (red), Lyve1 (green), and podoplanin (yellow). *A* shows a group of T cells at the sectioned surface of the nerve bundles (short arrows) suggesting an accumulation of T cells under the perineurium covering the nerve. One branch of the fifth cranial nerve is labeled with the roman numeral V. *B* demonstrates the colocalization of two lymphatic markers (podoplanin and Lyve1) in the endoneurial connective tissue and shows T cells (arrows) next to double-stained membranes. In *C*, yellow color represents PDPN, and the area where the red (CD3-positive) T cells gather is also strongly expressing the adhesion molecule ICAM1 (shown in green). A few PDPN-expressing cells with elongated nuclei are pointed at with arrows. ICAM1 seems to be expressed in the proximity of T cells. In *D*, the cross-section of the trigeminal ganglion and trigeminal branches from a strangulated victim is shown to demonstrate the T cell accumulation. Triple staining shows podoplanin (in white); ICAM1, the adhesion molecule known to be involved in T cell adhesion/migration (in green); and CD3 (in red) labeling all T cells. Large ganglion cells (some are labeled with stars) are clearly visible among the fibers. Note that—similarly to Fig. 7—only some of the ganglion cells are surrounded by ICAM1-positive green satellite cells (some of these are pointed out by arrows), while all other satellite cells are unstained for ICAM1 but still stained with PDPN (in yellow). (Scale bars: *A* and *D*, 100 μm; *B* and *C*, 50 μm.)

Semmelweis University, Budapest, Hungary, and additional trigeminal ganglia were obtained from the Maryland Tissue Bank. The paraffin-embedded blocks from the McLean Hospital were accompanied by descriptions of the neuropathology, and we selected areas least affected by disease for processing. In Hungary, the brains were dissected and a variety of brain areas, meninges, sinus cavernous, and brainstem with cranial nerves were isolated. The samples of the "cavernous sinus" were cut out from the dura at the medial part of the middle cranial fossa including nerves and vessels and also the posteriorly connected cavum trigeminale (Meckeli) with the trigeminal ganglion (Gasseri) and nerve branches. They were either flash frozen or embedded in paraffin after formalin fixation. The study was approved by European ethics regulations under permission TUKEB #189/2015. Frozen human trigeminal ganglia were donated by the Human Brain and Spinal Fluid Resource Center and collected from unidentified donors between the ages of 53 to 85 y. Postmortem times before autopsy varied from 2.2 to 24 h. Table 1 shows the samples that we examined and describe in the present paper.

Immunohistochemistry. The paraffin-embedded sections were deparaffinized with Safeclear II (Fisher Scientific; #044-192) and rehydrated in decreasing concentrations of ethanol immediately followed by heat-induced epitope retrieval (HIER) in 10 mM citrate buffer at pH 6.0 using a commercial microwave oven. Slides were placed in a microwave lying flat in a container and covered with the citrate buffer. They were brought to boil on high power (700 W), and then cooked for 5 more minutes at 50% power (350 W). After HIER, the slides were allowed to cool to room temperature in the buffer. Next, Bloxall (Vector; SP-6000) dual endogenous enzyme blocking solution was applied to all sections for 15 min before the primary antibodies were applied. We used a multiplex labeling method based on signal amplification and fluorescent tyramide dyes (29). The advantage of this technique is that antibodies from the same species can be used consecutively because the tyramide-conjugated fluorescent dye is insoluble in water allowing both the primary and secondary antibodies to be removed by heat. The fluorescent signal that comes from the insoluble tyramide complex remains where the target antigen is. This process can be replicated several

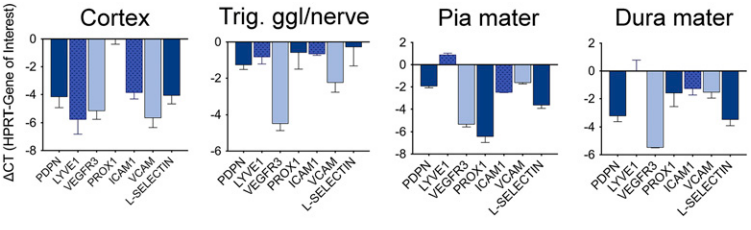

Fig. 9. qPCR analysis of the trigeminal ganglia and nerve, cortex, and meninges to confirm the presence of mRNA encoding the studied proteins. In samples from three different donors for the trigeminal samples and individual samples of other regions from the tissue that was used for ICC, the mRNAs encoding all the proteins that we visualized using immunostaining were also present, confirming their expression.

Table 1. Donor samples used in the study

Subject	Cause of death	PM time, h	Age	Gender
1	Strangulated	8	72	M
2*	Alzheimer's disease	2.2	74	M
3*	Infarcts/control block	12.8	80	F
4*	Pick's disease	22.75	65	F
5	Strangulated	11	85	M
6	Sleeping pill overdose	5	47	F
7	Pulmonary embolus	24	71	M
8*	Lewy body disease	23.6	71	M
9*	Alzheimer's disease	11.5	87	F
10*	Huntington's disease	14.3	67	F

Samples labeled with an asterisk were provided by the McLean Hospital. Unlabeled ones came from the Semmelweis University in Budapest, Hungary. PM, postmortem.

times using different fluorochromes conjugated to tyramide. The fluorescent signal emitted by the HRP–tyramide complex is significantly stronger than the one a traditional fluorochrome-conjugated secondary antibody gives. Briefly, the slides were incubated overnight at 4 °C with the first primary antibody followed by an anti-IgG of the appropriate species. These IgGs were preconjugated to an HRP polymer (VisUCyte HRP polymer; R&D Systems). The signal was then visualized by adding different color fluorochrome tyramide conjugates, which are high-affinity substrates of the HRP. After staining with the first primary antibody, the microwave cycle was repeated, leaving only one specific tyramide signal. Then additional primary antibodies (and fluorochrome tyramide conjugates) were used one after another. Finally, the different fluorochrome tyramides were visualized. For control staining, the primary antibody was omitted, but the amplification process including the incubation with the HRP-polymers and the tyramide-fluorochromes were unchanged. After completion of the procedure, all sections were counterstained with Sudan-black to quench autofluorescence due to lipofuscin and then analyzed with a Leica DMI6000 inverted fluorescent microscope using LAX software. More details on the staining and the source and use conditions of the antibodies are listed in *SI Appendix*, Table S1.

PCR from Cortex, Trigeminal Ganglia and Nerve, and Meninges. To extract RNA from them, frozen postmortem human cortex, meninges (from the same blocks that sections for ICC were cut), trigeminal ganglia, and nerve samples were powdered using a mortar and pestle and homogenized in TRIzol solution (Invitrogen) with a Dounce homogenizer. The RNA produced was assayed and assessed for quality using Nanodrop device. cDNA libraries were synthesized using a High-Capacity cDNA Reverse Transcription Kit (Applied Biosystems) according to the manufacturer's instructions. mRNAs were quantitated by means of real-time PCR using a SensiFast SYBR Hi-ROX Kit (Bioline) with its recommended run program in a StepOnePlus real-time PCR system (Applied Biosystems). HPRT1 was used as the reference gene for normalization. Thermo-cycling was performed in an Applied Biosystems StepOnePlus instrument: 2 min of initial heat activation at 95 °C, followed by 40 cycles of 5-s denaturation at 95 °C and 10-s combined annealing and extension at 60 °C. A final melt curve confirmed completion of the reactions. Data were analyzed with the StepOnePlus software, normalized to the housekeeping gene (HPRT). No template controls were run for each primer set. Double delta CT calculations were performed to determine fold changes. The custom-designed primers used in the real-time PCR are shown in *SI Appendix* (list of primer sequences).

Data Availability. All study data are included in the article and *SI Appendix*.

ACKNOWLEDGMENTS. This study was supported by the Intramural Research Program of the National Institute of Dental and Craniofacial Research (NIDCR), NIH (intramural project no. ZDE000755-01), and the Human Brain Bank, Semmelweis University Medical School, Hungary. We acknowledge the patients who donated their tissues from the McLean Brain Collection and from Hungary for postmortem examinations. We thank Ms. Maria Bakó (Department of Anatomy, Histology, and Embryology, Semmelweiss University) for her help with tissue processing. We are very grateful to Ms. Sharon Key for her initial work in optimizing the combination ICC techniques. Special thanks to Ms. Li Li (NIDCR) for her expert processing of the paraffin-embedded tissues. We thank Ms. Magdolna Toronyay-Kasztner for her outstanding help with putting the manuscript and the long list of old references together. We are very grateful to Dr. Michael Brownstein for editing the manuscript. We acknowledge Prof. Endre Csanda (deceased 5 years ago) and Prof. Samuel Komoly (University of Pécs Medical School) for thoughtful and creative discussions of the lymphatics and the brain over the last decade. Finally, we are grateful to all scientists across many centuries who devoted their time, thoughts, and life to solve one of nature's many puzzles using significantly less advanced techniques than we have at present. With modern methods, we can do little more than confirm their results decades (or centuries) later.

1. E. Crivellato, L. Travan, D. Ribatti, The Hippocratic treatise "On glands": The first document on lymphoid tissue and lymph nodes. *Leukemia* **21**, 591–592 (2007).
2. P. Mascagni, *Vasorum Lymphaticorum Corporis Humani Descriptio e Iconographia* (Pazzini Carli, Siena, Italy, 1787).
3. G. Schwalbe, Der Arachnoidealraum, ein Lymphraum und sein Zusammenhang mit dem Perichorioidealraum. *Centralblatt für die medicinischen Wissenschaften* **7**, 465 (1869).
4. A. Key, G. Retzius, *Studien in der Anatomie des Nervensystems und des Bindegewebes* (Samson und Wallin, Stockholm, 1875).
5. J. B. Tuke, The Morisonian Lectures, delivered before the Royal College of Physicians of Edinburgh: Session 1874. *Edinburgh Med. J.* **20**, 687–700 (1875).
6. A. Bruce, J. W. Dawson, On the relations of the lymphatics of the spinal cord. *J. Pathol. Bacteriol.* **15**, 169–178 (1911).
7. H. Obersteiner, *The Anatomy of the Central Nervous Organs in Health and Disease* (Charles Griffin, London, 1900), pp. 174–175.
8. H. Zwillinger, Die Lymphbahnen des oberen Nasalschnittes und deren Beziehungen zu den perimeningealen Lymphraumen. *Arch. Laryngol. und Rhinol.* **26**, 66–78 (1912).
9. R. T. Jackson, J. Tigges, W. Arnold, Subarachnoid space of the CNS, nasal mucosa, and lymphatic system. *Arch. Otolaryngol.* **105**, 180–184 (1979).
10. J. B. Brierley, E. J. Field, The connexions of the spinal sub-arachnoid space with the lymphatic system. *J. Anat.* **82**, 153–166 (1948).
11. L. Koh, A. Zakharov, M. Johnston, Integration of the subarachnoid space and lymphatics: Is it time to embrace a new concept of cerebrospinal fluid absorption? *Cerebrospinal Fluid Res.* **2**, 6 (2005).
12. M. Földi *et al*., New contributions to the anatomical connections of the brain and the lymphatic system. *Acta Anat. (Basel)* **64**, 498–505 (1966).
13. E. Csanda, F. Obál, F. J. Obál, "Central nervous system and lymphatic system" in *Lymphangiology*, M. Földi, J. R. Casley-Smith, Eds. (Schattauer, Stuttgart, 1983), pp. 475–508.
14. E. Csanda, T. O. Zoltan, M. Foldi, Elevation of cerebrospinal-fluid pressure in the dog after obstruction of cervical lymphatic channels. *Lancet* **1**, 832 (1963).
15. H. F. Cserr, C. J. Harling-Berg, P. M. Knopf, Drainage of brain extracellular fluid into blood and deep cervical lymph and its immunological significance. *Brain Pathol.* **2**, 269–276 (1992).
16. M. Földi, The brain and the lymphatic system revisited. *Lymphology* **32**, 40–44 (1999).
17. H. Benveniste, H. Lee, N. D. Volkow, The glymphatic pathway: Waste removal from the CNS via cerebrospinal fluid transport. *Neuroscientist* **23**, 454–465 (2017).
18. J. J. Iliff, M. Nedergaard, Is there a cerebral lymphatic system? *Stroke* **44**(suppl. 1): S93–S95 (2013).
19. N. A. Jessen, A. S. Munk, I. Lundgaard, M. Nedergaard, The glymphatic system: A beginner's guide. *Neurochem. Res.* **40**, 2583–2599 (2015).
20. R. O. Weller, E. Djuanda, H. Y. Yow, R. O. Carare, Lymphatic drainage of the brain and the pathophysiology of neurological disease. *Acta Neuropathol.* **117**, 1–14 (2009).
21. B. A. Plog, M. Nedergaard, The glymphatic system in central nervous system health and disease: Past, present, and future. *Annu. Rev. Pathol.* **13**, 379–394 (2018).
22. M. Johnston, D. Armstrong, L. Koh, Possible role of the cavernous sinus veins in cerebrospinal fluid absorption. *Cerebrospinal Fluid Res.* **4**, 3 (2007).
23. J. Ramirez *et al*., Imaging the perivascular space as a potential biomarker of neurovascular and neurodegenerative diseases. *Cell. Mol. Neurobiol.* **36**, 289–299 (2016).
24. A. Aspelund *et al*., A dural lymphatic vascular system that drains brain interstitial fluid and macromolecules. *J. Exp. Med.* **212**, 991–999 (2015).
25. A. Louveau *et al*., Structural and functional features of central nervous system lymphatic vessels. *Nature* **523**, 337–341 (2015).
26. M. Absinta *et al*., Human and nonhuman primate meninges harbor lymphatic vessels that can be visualized noninvasively by MRI. *eLife* **6**, e29738 (2017).
27. G. Ringstad, P. K. Eide, Cerebrospinal fluid tracer efflux to parasagittal dura in humans. *Nat. Commun.* **11**, 354 (2020).
28. Y. Meng *et al*., Glymphatics visualization after focused ultrasound-induced blood-brain barrier opening in humans. *Ann. Neurol.* **86**, 975–980 (2019).
29. Z. E. Tóth, E. Mezey, Simultaneous visualization of multiple antigens with tyramide signal amplification using antibodies from the same species. *J. Histochem. Cytochem.* **55**, 545–554 (2007).
30. J. S. Choi *et al*., Expression of vascular endothelial growth factor receptor-3 mRNA in the rat developing forebrain and retina. *J. Comp. Neurol.* **518**, 1064–1081 (2010).
31. Y. Hou *et al*., Expression of vascular endothelial growth factor receptor-3 mRNA in the developing rat cerebellum. *Cell. Mol. Neurobiol.* **31**, 7–16 (2011).
32. Y. J. Shin, T. R. Riew, J. H. Park, H. J. Pak, M. Y. Lee, Expression of vascular endothelial growth factor-C (VEGF-C) and its receptor (VEGFR-3) in the glial reaction elicited by human mesenchymal stem cell engraftment in the normal rat brain. *J. Histochem. Cytochem.* **63**, 170–180 (2015).

NEUROSCIENCE

33. F. J. Sun *et al*., Elevated expression of VEGF-C and its receptors, VEGFR-2 and VEGFR-3, in patients with mesial temporal lobe epilepsy. *J. Mol. Neurosci.* **59**, 241–250 (2016).
34. J. Pedragosa *et al*., CNS-border associated macrophages respond to acute ischemic stroke attracting granulocytes and promoting vascular leakage. *Acta Neuropathol. Commun.* **6**, 76 (2018).
35. M. Hutchings, R. O. Weller, Anatomical relationships of the pia mater to cerebral blood vessels in man. *J. Neurosurg.* **65**, 316–325 (1986).
36. A. W. Morris *et al*., Vascular basement membranes as pathways for the passage of fluid into and out of the brain. *Acta Neuropathol.* **131**, 725–736 (2016).
37. E. T. Zhang, C. B. Inman, R. O. Weller, Interrelationships of the pia mater and the perivascular (Virchow-Robin) spaces in the human cerebrum. *J. Anat.* **170**, 111–123 (1990).
38. B. Engelhardt, P. Vajkoczy, R. O. Weller, The movers and shapers in immune privilege of the CNS. *Nat. Immunol.* **18**, 123–131 (2017).
39. R. Pestalozzi, *Ober Aneurysmataspuriaderkleinen Gehirnarterienundihren Zuzammenhang mit Apoplexie* (F. E. Thein, Wurtzburg, 1849).
40. R. Virchow, Tiber die Erweiterung kleinerer Gefasse. *Virchows Arch.* **3**, 427–462 (1851).
41. C. Robin, Recherches sur quelques particularities de la structure des capillaires de l'encephale l'homme. *J. Physiol.* **2**, 536–548 (1859).
42. F. W. Mott, M. D. Lond, F. R. C. P. Lond, The Oliver-Sharpey lectures on the cerebrospinal fluid. *Lancet* **176**, 1–8 (1910).
43. D. H. Woollam, J. W. Millen, The perivascular spaces of the mammalian central nervous system and their relation to the perineuronal and subarachnoid spaces. *J. Anat.* **89**, 193–200 (1955).
44. H. F. Cserr, D. N. Cooper, T. H. Milhorat, "Production, circulation and absorption of brain interstitial fluid" in *Dynamics of Brain Edema*, H. M. Pappius, W. Feindel, Eds. (Springer, Berlin, 1976), pp. 95–97.
45. M. Földi, B. Csillik, O. T. Zoltán, Lymphatic drainage of the brain. *Experientia* **24**, 1283–1287 (1968).
46. E. Csanda *et al*., Structural, ultrastructural and functional reactions of the brain after implanting yttrium 90 rods used in stereotactic neurosurgery. *Acta Neurochir. (Wien)*, **1977** (suppl. 24), 139–147 (1977).
47. K. H. Andres, M. von Düring, K. Muszynski, R. F. Schmidt, Nerve fibres and their terminals of the dura mater encephali of the rat. *Anat. Embryol. (Berl.)* **175**, 289–301 (1987).
48. S. Podgrabinska *et al*., Molecular characterization of lymphatic endothelial cells. *Proc. Natl. Acad. Sci. U.S.A.* **99**, 16069–16074 (2002).
49. E. Ellwardt, J. T. Walsh, J. Kipnis, F. Zipp, Understanding the role of T cells in CNS homeostasis. *Trends Immunol.* **37**, 154–165 (2016).
50. S. S. Ousman, P. Kubes, Immune surveillance in the central nervous system. *Nat. Neurosci.* **15**, 1096–1101 (2012).
51. W. F. Hickey, Leukocyte traffic in the central nervous system: The participants and their roles. *Semin. Immunol.* **11**, 125–137 (1999).
52. S. Kida, P. V. Steart, E. T. Zhang, R. O. Weller, Perivascular cells act as scavengers in the cerebral perivascular spaces and remain distinct from pericytes, microglia and macrophages. *Acta Neuropathol.* **85**, 646–652 (1993).
53. C. Harling-Berg, P. M. Knopf, J. Merriam, H. F. Cserr, Role of cervical lymph nodes in the systemic humoral immune response to human serum albumin microinfused into rat cerebrospinal fluid. *J. Neuroimmunol.* **25**, 185–193 (1989).
54. P. Kivisäkk, B. Tucky, T. Wei, J. J. Campbell, R. M. Ransohoff, Human cerebrospinal fluid contains $CD4^+$ memory T cells expressing gut- or skin-specific trafficking determinants: Relevance for immunotherapy. *BMC Immunol.* **7**, 14 (2006).
55. I. Galea, I. Bechmann, V. H. Perry, What is immune privilege (not)? *Trends Immunol.* **28**, 12–18 (2007).
56. M. Prinz, J. Priller, The role of peripheral immune cells in the CNS in steady state and disease. *Nat. Neurosci.* **20**, 136–144 (2017).
57. A. Svenningsson *et al*., Adhesion molecule expression on cerebrospinal fluid T lymphocytes: Evidence for common recruitment mechanisms in multiple sclerosis, aseptic meningitis, and normal controls. *Ann. Neurol.* **34**, 155–161 (1993).
58. R. Lyck *et al*., T-cell interaction with ICAM-1/ICAM-2 double-deficient brain endothelium in vitro: The cytoplasmic tail of endothelial ICAM-1 is necessary for transendothelial migration of T cells. *Blood* **102**, 3675–3683 (2003).
59. E. N. Marieb, K. Hoehn, *Human Anatomy and Physiology* (Benjamin Cummings, San Francisco, 2009).
60. R. A. Sobel, M. E. Mitchell, G. Fondren, Intercellular adhesion molecule-1 (ICAM-1) in cellular immune reactions in the human central nervous system. *Am. J. Pathol.* **136**, 1309–1316 (1990).
61. B. Engelhardt, R. M. Ransohoff, The ins and outs of T-lymphocyte trafficking to the CNS: Anatomical sites and molecular mechanisms. *Trends Immunol.* **26**, 485–495 (2005).
62. J. Greenwood *et al*., Intracellular domain of brain endothelial intercellular adhesion molecule-1 is essential for T lymphocyte-mediated signaling and migration. *J. Immunol.* **171**, 2099–2108 (2003).
63. E. Csanda, M. Földi, F. Obál, O. T. Zoltán, Cerebral oedema as a consequence of experimental cervical lymphatic blockage. *Angiologica* **5**, 55–63 (1968).
64. J. H. Ahn *et al*., Meningeal lymphatic vessels at the skull base drain cerebrospinal fluid. *Nature* **572**, 62–66 (2019).
65. J. Goldmann *et al*., T cells traffic from brain to cervical lymph nodes via the cribroid plate and the nasal mucosa. *J. Leukoc. Biol.* **80**, 797–801 (2006).
66. J. G. Veening, H. P. Barendregt, The regulation of brain states by neuroactive substances distributed via the cerebrospinal fluid; a review. *Cerebrospinal Fluid Res.* **7**, 1 (2010).
67. E. Song *et al*., VEGF-C-driven lymphatic drainage enables immunosurveillance of brain tumours. *Nature* **577**, 689–694 (2020).
68. M. Johnston, C. Papaiconomou, Cerebrospinal fluid transport: A lymphatic perspective. *News Physiol. Sci.* **17**, 227–230 (2002).
69. J. B. Tuke, The Morisonian Lectures, delivered before the Royal College of Physicians of Edinburgh: Session 1894. *Edinburgh Med. J.* **39**, 673–683 (1894).
70. J. B. Tuke, Note on the anatomy of the pia mater. *Trans. Med. Chir. Soc. Edinb.* **1**, 118–122 (1882).
71. J. J. Iliff *et al*., A paravascular pathway facilitates CSF flow through the brain parenchyma and the clearance of interstitial solutes, including amyloid β. *Sci. Transl. Med.* **4**, 147ra111 (2012).
72. K. M. Charlton, M. M. Garcia, Spontaneous listeric encephalitis and neuritis in sheep. Light microscopic studies. *Vet. Pathol.* **14**, 297–313 (1977).
73. J. L. Thomas, L. Jacob, L. Boisserand, [Lymphatic system in central nervous system] [in French]. *Med. Sci. (Paris)* **35**, 55–61 (2019).
74. E. Raz *et al*., Possible empirical evidence of glymphatic system on computed tomography after endovascular perforations. *World Neurosurg.* **134**, e400–e404 (2020).
75. S. Naganawa, R. Ito, T. Taoka, T. Yoshida, M. Sone, The space between the pial sheath and the cortical venous wall may connect to the meningeal lymphatics. *Magn. Reson. Med. Sci.* **19**, 1–4 (2020).